

SECTION-III

CHAPTER 3.

RESULTS AND DISCUSSION

3. RESULTS AND DISCUSSION

As envisaged it was planned to identify potential new heterocyclic compounds useful in treatment of neurodegenerative disorders. A strategy of exploring multiple chemical templates containing cyclic guanidine skeleton in common, was adopted, in order to enhance success rate of the compounds for advanced biological studies. Since acetylcholine level plays a major role for the accumulation of amyloid-beta plaque in the brain of patients having AD, the approach was adapted to design and synthesize heterocyclic templates having dual activity as cholinesterase inhibitors and beta-amyloid aggregation inhibitors.

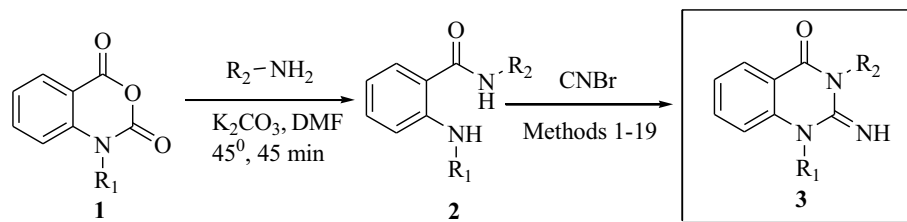
The following section has been divided into two parts- one for chemical studies and the other for biological studies.

3.1. Chemical studies

The use of room temperature ionic liquids (RTILs) as solvents or catalysts for chemical reactions offers several advantages from the environmental perspective. Therefore, RTILs⁶⁰ are attracting academic and industrial attention world wide,⁶¹ as these can be used to replace the organic solvents in catalysis,⁶² synthesis,^{63,64} and separations.⁶⁵ The unique properties of RTILs enable their use as alternative solvents and may speed up the introduction of potentially 'green' solvents in sustainable industrial processes.

Initially, synthesis of 2-imino-4-quinazolinones (**3**), cyclic guanidine derivatives was initiated using the reported processes. For the preparation of the target structure (**3**), substituted isatoic anhydride (**1**) was reacted with suitable primary amines to afford 2-aminobenzamides (**2**). It was planned to react the intermediate (**2**) with

cyanogen bromide to obtain the desired compound (**3**) (**Scheme 1**). Classical methods for the synthesis of cyclic guanidines typically require excess of cyanogen bromide in



Scheme 1

protic polar solvents like ethanol and activated diamines at higher temperatures.⁶⁶

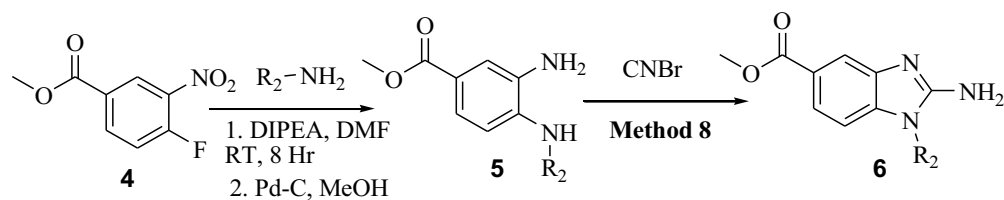
When the reaction of compound (**2**) was carried out in ethanol, it took 6-8 hr for the

Table 1. Synthesis of 1,3-disubstituted-2-imino-2,3-dihydroquinazolin-4-ones (**3**)

Entry	Substituents		Yield (%)		
	R ₁	R ₂	EtOH, 70° C, 6-8 hr	EtOH M.W. 150 W 90° C, 8-10 min	RTIL: DMSO (1:10) 90° C, 5-8 min
3ah	Me	CH ₂ CH ₂ CH ₂ CH ₃	78	89	90
3al	Me	Cyclohexyl	74	90	92
3bh	CH ₂ CH ₂ CH ₂ CH ₃	CH ₂ CH ₂ CH ₂ CH ₃	76	88	92
3bi	CH ₂ CH ₂ CH ₂ CH ₃	CH(CH ₃) ₂	82	90	94
3bm	CH ₂ CH ₂ CH ₂ CH ₃	CH ₂ CH ₂ Ph	65	85	88
3ch	CH ₂ CH ₂ CH ₂ CH ₃	CH ₂ CH ₂ CH ₂ CH ₃	72	92	95
3cl	CH ₂ CH ₂ CH ₂ CH ₃	Cyclohexyl	56	85	82
3cm	CH ₂ CH ₂ CH ₂ CH ₃	CH ₂ CH ₂ Ph	85	95	94
3dh	CH ₂ CH ₂ CH=CH ₂	CH ₂ CH ₂ CH ₂ CH ₃	73	90	94
3eh	CH ₂ CH ₂ CH ₂ CH ₃	CH ₂ CH ₂ CH ₂ CH ₃	72	89	90
3ei	CH ₂ CH ₂ CH ₂ CH ₃	CH(CH ₃) ₂	80	90	92
3el	CH ₂ CH ₂ CH ₂ CH ₃	Cyclohexyl	78	94	95
3es	CH ₂ CH ₂ CH ₂ CH ₃	CH ₂ CH ₂ Ph	74	90	92

reaction to complete, offering medium to good yields (**Table 1**). To further enhance the yields of the products (**3**), it was thought to carry out the reaction in polar aprotic solvents like dimethyl sulphoxide (DMSO) or in ILs like dibutylimidazolium bromide ([bbim]⁺[Br]⁻). Surprisingly in pure DMSO or in pure IL, the desired products could not be obtained even after heating of the reaction mixtures for 12 hr at 90 °C. There are some reports⁶⁷⁻⁶⁹ of catalyzing effects of IL in DMSO on some reactions. Srinivasan et. al. have reported a facile esterification reaction using sodium carboxylates and alkyl halides in 1:10 ratio of RTIL and DMSO.^{70,71} Thinking that this ratio might work with our reactants, the reaction was repeated using the same ratio of IL and DMSO at 90 °C. To our astonishment the ratio of 1:10 of IL and DMSO offered the desired products in high yields in a short span of time (5-8 min). Cyclization was also tried under microwave irradiation. Exposure of the reaction mixture with brief period to microwaves offered the desired products in high yields.

Results depicted in **Table 1** are quite evident to show that these protocols could be adopted for the synthesis of various aromatic heterocycles. In order to expand the

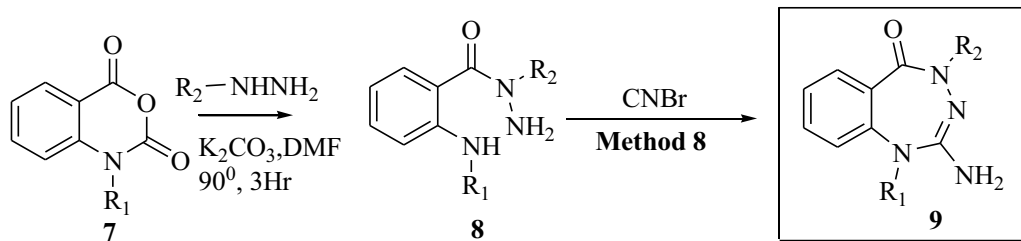


Scheme 2

Table 2. Synthesis of 1-substituted-2-aminoimidazoles (**6**)

Entry	Substituent (R ₂)	Yield(%)		
		EtOH, 70° C, 6-8 hr	EtOH, M.W. 150W 90° C, 8-10 min	RTIL: DMSO (1:10) 90° C, 5-8 min
6o		70	92	94
6n		84	94	95
6s		72	88	89

diversity profile of the resulting cyclic guanidines, synthesis of five and seven membered benzo-annelated systems like 2-aminoimidazole and 2-aminobenzo-1,2,4-triazepin-5-one were also investigated. Results of RTIL-DMSO protocol and microwave irradiation methods are shown in **Table 2** and **Table 3**. Synthesis of 2-aminoimidazole (**6**) was started with methyl 4-fluoro-2-nitrobenzoate



Scheme 3



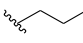
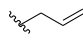
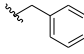
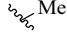
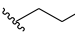
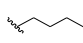
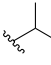
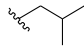

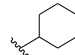
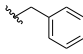
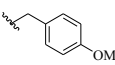
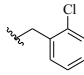
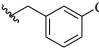
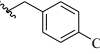
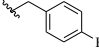
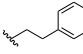
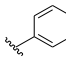
Table 3. 1,4-disubstituted-1,2,3,4-tetrahydro-2-aminobenzo-1,2,4-triazepin-5-one (**9**)

Entry	Substituents		Yield%		
	R ₁	R ₃	EtOH, 70° C, 6-8 hr	EtOH M.W. 150W 90° C, 8-10 min	RTIL: DMSO (1:10) 90° C, 5-8 min
9ct			54	82	90
9es			68	90	92

and carried out in three steps; nucleophilic substitution with suitable amines, reduction of nitro group and cyclization with CNBr in RTIL and separately by microwave irradiation, offering **6** in good yields (**Scheme 2**). Consequently, the synthesis of 2-aminobenzotriazepin-5-one was also achieved, starting with N-substituted isatoic anhydride by using the same protocol as described above (**Scheme 3**).

After improving the yields of the desired benzo-annelated cyclic guanidines it was thought of reducing the reaction temperature so that the developed experimental protocol could be applied to temperature-sensitive starting materials. Replacing ethanol with easily available methanol proved disastrous as the reaction mixture did

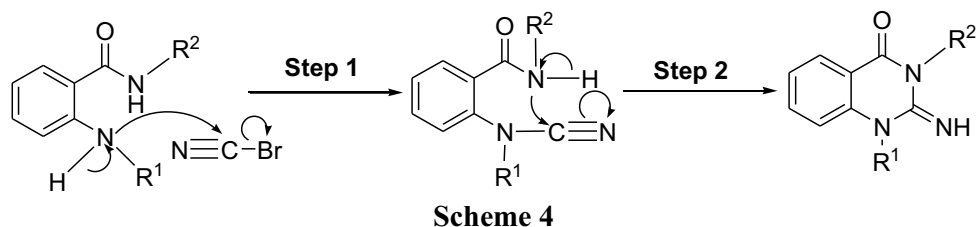
Table 4. Substituents used for the synthesis of cyclic guanidine derivatives (**3**, **6** & **9**)

$R_1=$	 a	 b	 c	 d	 e
$R_2=$	 f	 g	 h	 i	 j
	 k	 l	 m	 n	 o
	 p	 q	 r	 s	 t

not proceed even after refluxing the reaction mixture for 18 hr. Here also the IL:DMSO mixture in 1:10 ratio provided another pleasant surprise when the reaction got completed in just 25 minutes at room temperature to afford a high quality product (**3el**) in high yields (**Table 5**). The quality of the product was so good that simple dilution of the reaction mixture with ice-water, filtration and water washing of the precipitate yielded analytical grade sample. Thinking that a simple mixture of both these solvents would yield same results, different ratios of IL-DMSO were also explored as solvent. Different concentrations of IL like 5%, 10%, 20%, 30% and 50% in DMSO were used to observe the results. Among all of these ratios an optimum 10-20% IL in DMSO gave the best results and the reaction was completed in 25-30 min at room temperature. By decreasing or increasing the ratio of IL in DMSO it took more time (2-8 hr) to complete the reaction. Use of 10% IL in DMSO at room temperature was of special interest to us as this protocol could be adopted for temperature sensitive compounds with low concentrations of costly ILs. As the aim of the study was to synthesise sufficient number of compounds having enough diversity,

the IL-DMSO (1:10) protocol (**method 8**) was used as a common method for the synthesis of nearly 70 derivatives of 2-iminoquinazolinone (**3**) scaffold. All the synthesized compounds were then screened for their biological activities.

The above described observations needed a plausible explanation. During the course of reactions using various solvents under different temperature conditions, it was observed that the reaction proceeds in two steps (**Scheme 4**) as inferred from the TLC analysis of the reaction mixtures, when analysed at different time intervals. It became evident that **Step 1** is a slower one than **Step 2**. That means IL-DMSO mixture (1:10) might be catalysing both the steps but definitely does catalyze **Step 1**. **Step 1** can be considered to be nucleophilic substitution reaction while **Step 2** is essentially an addition step. Transition state of **Step 1** is expected to be much more



highly polarized than the starting reactants. Factors leading to stabilization of the transition state would enhance the rate of reaction in **Step 1**.

A high level of stabilization of the transition state can be explained by a mixture of DMSO and IL as shown in **Figure 5**. IL and DMSO make two pseudo ring structures with both of the reacting species thereby stabilizing the partial charges on the atoms as shown in **Figure 5**. Formation of ring (A) increases the nucleophilicity of amino nitrogen by increasing the partial negative charge through hydrogen bonding with oxygen of DMSO and stabilising the developing negative charge on nitrogen of cyano group through electrostatic interaction with sulphur of DMSO. Formation of

ring (**B**) is much more important as it would stabilize the developing negative charge on bromine and nitrogen atoms through hydrogen bonding with the two planar

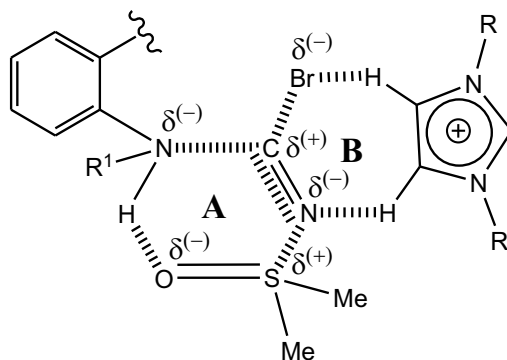


Figure 5

hydrogens of $[\text{bbim}]^+$.^{72,73} As carbon and nitrogen atoms of cyanogen bromide would be in a state similar to sp^2 hybridization state, formation of a planar pseudo seven-

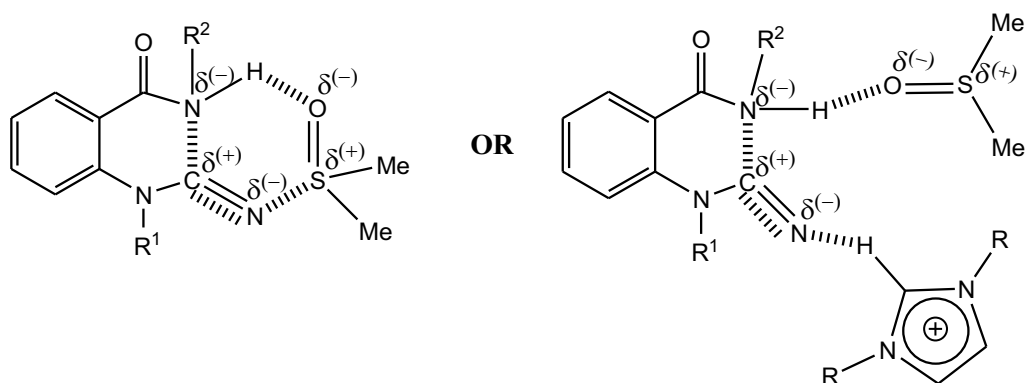


Figure 6

membered ring (**B**) would be stable in the transition state. Once the cyanamide intermediate is formed, **Step 2** is expected to be quite fast as an intra-molecular addition reaction takes place. There could be some degree of stabilization of the transition state by DMSO in **Step 2** also, as seen in **Figure 6**. This stabilization could be facilitated by DMSO either all alone or in conjugation with IL. Either of the acidic protons^{29,30} of C-2, C-4 or C-5 of IL can participate in stabilization of this transition

state. But the overriding factor seems to be the internal attack of the nucleophile in **Step 2**. As the reaction rate is observed to be slower in other proportions of IL and DMSO than 10-20%, it is hypothesized that higher or lower concentrations of IL in DMSO disrupts the matrix as shown in the **Figure 5** in the transition state of **Step 1** rather than affecting the transition state of **Step 2**.

Since the developing negative charges on bromide and nitrogen atoms in the transition stage (**Step 2**) could be stabilized by a cation through electrostatic interaction, it was considered worthwhile to perform the reaction in presence of salts

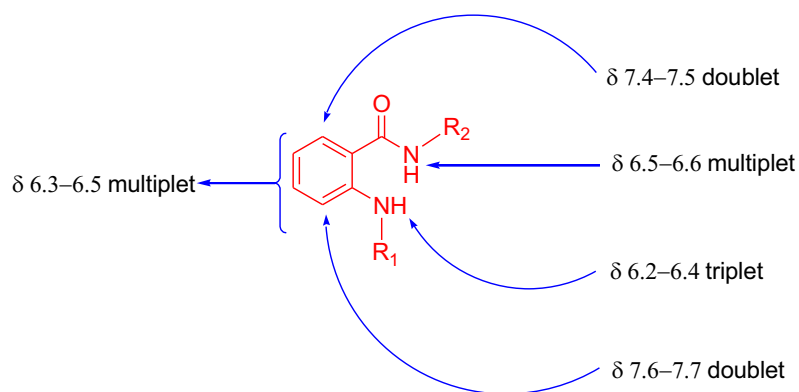
Table 5. Formation of compound (**3el**) using different synthetic methods

Method	Solvent/ Reaction cond.	Temp. °C	Compound (3el)	
			Time	Yield (%)
1.	EtOH	reflux	8 h	70
2.	EtOH	RT	18 h	60
3.	MeOH	RT/reflux	18 h	no rean.
4.	Toluene	reflux	12 h	no rean.
5.	DMSO	RT/reflux	28 h	58
6.	IL	RT/90	18 h	52
7.	IL:DMSO::1:10	RT	25 min	94
8.	IL:DMSO::1:10	90	8 min	93
9.	IL:DMSO:: 1:1	RT	5 h	85
10.	KBr+DMSO	RT	45 min	86
11.	CsBr+DMSO	RT	4 h	82
12.	NaBr+DMSO	RT	6 h	84
13.	LiBr+DMSO	RT	12 h	82
14.	KCl+DMSO	RT	1 h	88
15.	KI+DMSO	RT	16 h	62
16.	Cs ₂ CO ₃ +DMSO	RT	18 h	no rean.
17.	Cu ₂ I ₂ +DMSO	RT	18 h	no rean.
18.	KBr+IL	RT	18 h	53
19.	EtOH+M.W.	reflux	5 min	92

with varying sizes of cations in the reaction medium having DMSO as the solvent. As solvation factor of the cation and/or the anion could be an important criterion in catalytic reactions, anions of varying sizes were employed in the salts. To compare and establish the facts, a representative compound of 6-membered cyclic guanidine derivative (**3el**) was synthesized using different salts and maintaining reaction conditions as mentioned above. The results are summarized in **Table 5**. These results show that the use of potassium bromide in DMSO afforded the product fastest while iodide was the least effective amongst the potassium salts of halides. Being a much bigger cation cesium bromide was expected to give the product fastest but it catalyzed the reaction slower than the potassium ions. Among the halides of potassium salts, iodide was even poorer than chloride. This might be due to lesser degree of solvation of iodide than chloride or bromide, leading to existence of higher concentrations of potassium iodide as tighter ion pair than that of chloride or bromide ion pairs with potassium ions. Potassium bromide in pure IL was not very effective in catalysing the reaction, as was expected. The cyclization reaction rate was enhanced in ethanol also by microwave irradiation. In microwave reaction conditions, stabilization of the transition state in **Step 1** is not that very important factor because requisite energy could efficiently be delivered to the reacting species to cross the energy barrier in the transition state.

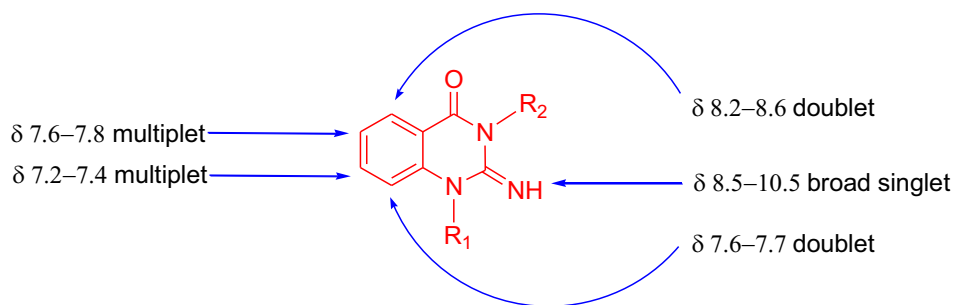
A mild, convenient and efficient protocol for the synthesis of benzo-annelated cyclic guanidines like 2-aminobenzimidazole (**6**), 2-imino-4-quinazolinone (**3**) and 2-aminobenzotriazepin-5-one (**9**) has been established by using diamine, amine and amide derivatives respectively, and cyanogen bromide in a mixture of IL in DMSO (1:10 ratio). As all of the synthesized compounds were novel and new, they were

characterized by using different spectral techniques viz. IR, ^1H -NMR and mass spectroscopy. Apart from the final compounds (3) synthesized in **scheme 1**, many of the intermediate compounds (2) were unknown and their structure resemblance with betrixaban (a potent anti-thrombotic agent currently in advance phase of clinical trials) was of much interest to design and develop them as a potent antithrombotic agents. As a part of confirmation of structures of unknown motifs, derivatives of compound (2) were also characterized by using different analytical techniques viz. IR, ^1H -NMR and mass spectroscopy. Purity of the compounds was established by TLC and elemental analysis. The characteristic ^1H -NMR spectrum of derivatives of compound (2) showed protons in aromatic ring at α -positions as doublet in the range of δ 7.4-7.5 and δ 7.6 to 7.7; other two protons of aromatic ring appeared as multiplets in the range of δ 6.3-6.5. Proton of amidic nitrogen appeared in the range of δ 6.5-6.6 as multiplet and proton of amine nitrogen appeared in the range of δ 6.2-6.4 as a triplet. In FT-IR spectrum amine functional group of compound (2) appeared in the range of 3370-3398 cm^{-1} as a medium single peak and aromatic $=\text{C}-\text{H}$ stretching in the range of 3000-3100 cm^{-1} . The amide $\text{C}=\text{O}$ appeared in the range of 1620-1640 cm^{-1} . For *Ortho*-disubstituted aromatic ring, $=\text{C}-\text{H}$ bending appeared in the range of 740-750 cm^{-1} .



^1H -NMR values of 2-aminobenzamide derivatives (2)

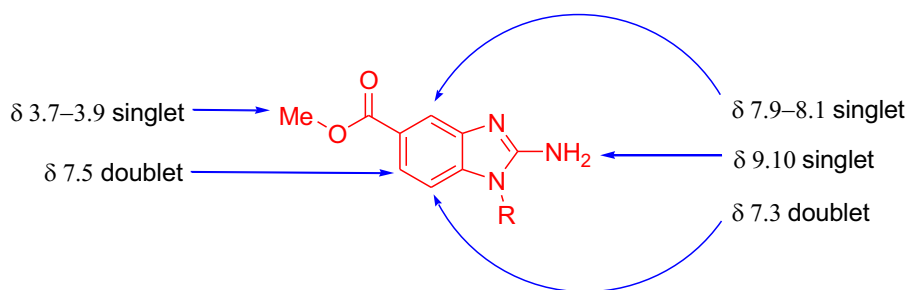
For compound (3) the $^1\text{H-NMR}$ peak of imine proton appeared in the range of δ 8.5-10.5. Aromatic protons appeared separately, one as a doublet in the range of δ 8.2-8.6 and another also as a doublet in the range of δ 7.6-7.7. The other two aromatic protons appeared as multiplets in the range of δ 7.6-7.8 and δ 7.2-7.4 respectively. In



$^1\text{H-NMR}$ values of 2-imino-4-quinazolinone derivatives (3)

FT-IR spectrum, NH stretching appeared in the range of $3300\text{--}3450\text{ cm}^{-1}$ and imine stretching in the range of $1680\text{--}1699\text{ cm}^{-1}$. Amide C=O stretching appeared in the range of $1640\text{--}1660\text{ cm}^{-1}$. Aromatic C=C stretching appeared at about 1617 cm^{-1} .

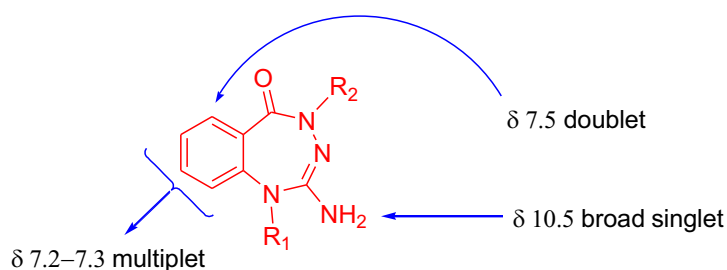
Similarly for the characterization of compound (6), spectral analysis has been performed and the $^1\text{H-NMR}$ peak for protons of primary amino of 2-aminobenzimidazole ring appeared at δ 9.10 as a singlet. One aromatic proton appeared in the range of δ 7.9-8.1 as a singlet and the other two protons appeared as



$^1\text{H-NMR}$ values of 2-aminobenzimidazole derivatives (6)

two different doublets at δ 7.5 and at δ 7.3 respectively. The methyl protons of ester functionality appeared in the range of δ 3.7-3.9 as a singlet. The prominent peaks in FT-IR spectrum of compound (6) contained NH stretching of amine in the range of 3300-3420 cm^{-1} , aromatic $=\text{C}-\text{H}$ stretching in the range of 3000-3100 cm^{-1} and ester $\text{C}=\text{O}$ stretching in the range of 1698-1720 cm^{-1} .

The seven-membered heterocyclic ring system, 2-aminotriazepine (9) was also characterized by using different spectral techniques. In ^1H -NMR spectrum, protons of guanidine nitrogen appeared at δ 10.5 as a broad singlet. As the protons of guanidine nitrogen are delocalized between two nitrogen atoms, a broad singlet was



^1H -NMR values of 2-amino-5-benzotriazepinone derivatives (9)

observed in ^1H -NMR spectrum. One proton of aromatic ring appeared at δ 7.5 as a doublet and the other three protons appeared in the range of δ 7.2-7.3 as multiplets. In the FT-IR spectrum guanidine NH_2 appeared at 3447 cm^{-1} , aromatic $=\text{C}-\text{H}$ stretching at 3128 cm^{-1} and amide $\text{C}=\text{O}$ at 1701. Purity of the synthesized compounds was confirmed by TLC and elemental analysis. As the guanidine derivatives were sensitive to column silica, all of them were purified by solvent precipitation and crystallization techniques.

3.2. Biological studies

As mentioned previously, the intermediate compounds (**2**) are new chemical entities and structurally resemble with potent anti-thrombotic agent betrixaban, it was planned to screen these compounds for their possible anti-thrombotic potency. Biological studies are hence divided into two parts: part A dealt with the planned screening of desired compounds (**3**, **6** and **9**) for their CNS-activity, on the other hand; part B explored the possibility of intermediate compounds (**2**) to become potent anti-thrombotic agents by testing them with suitable protocols of anti-thrombotic screening.

3.2.1. Part A-Anti-Alzheimer's activity

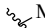
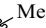
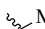


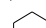
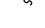


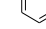
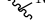
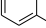





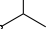


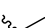


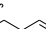

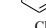



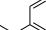

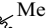



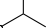
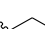
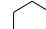

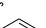

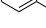
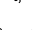
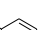





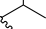
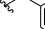
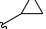
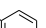
The characteristic hallmarks of AD include the rapid loss of cholinergic neurotransmission, accelerated aggregation of amyloid- β ($A\beta$) peptides and formation of neurofibrillary tangles (NFTs) of hyperphosphorylated tau-protein. These characteristics establish the basis for the cholinergic, amyloid and tau-hypotheses for AD pathology. According to the cholinergic hypothesis, the pathology of AD is attributed to the rapid decline in neurotransmission in the cholinergic regions of the CNS that house acetylcholine (ACh) utilizing sympathetic and parasympathetic neurons. The acetyl and butyrylcholinesterase (AChE and BuChE, respectively) enzymes act on ACh to terminate its actions in the synaptic cleft by hydrolyzing the neurotransmitter to choline and acetate.⁷⁴⁻⁷⁸ Deficiencies in the ACh synthesizing enzyme (choline acetyltransferase-ChAT) also contribute to the overall decline of ACh concentration in the cortical regions of the brain. Furthermore, recent studies have shown that the ratio of AChE to BuChE is dependent on the stage of

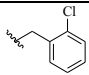
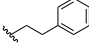
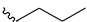
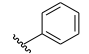
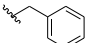
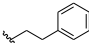
pathogenesis. In the CNS, AChE plays a vital role in the early stages of AD. However, as the disease progresses and cholinergic neurons are depleted, BuChE, which has a wider distribution within the body, acts as the major degrading enzyme.^{79,80} In contrast, the amyloid-hypothesis suggests that the progression of AD is attributed to the accelerated accumulation of toxic forms of self-induced and/or AChE-promoted toxic aggregates of A β peptides. These toxic peptides arise from the cleavage of the amyloid-precursor protein (APP) by the β -secretase (BACE-1) and γ -secretase enzymes. In this regard, recent studies indicate a link between the cholinergic and amyloid hypotheses.^{81,82} AChE is known to induce amyloid- β (A β) formation leading to the highly toxic AChE-A β peptide complexes.⁸³⁻⁸⁵ These multiple factors in AD pathology mandate the need to develop small molecule therapies that exhibit dual ChE inhibition as well as reduce the formation of neurotoxic A β -aggregates. With this aim the synthesized compounds were screened for ChE inhibition, *h*AChE-induced A β -aggregation inhibition and cytotoxicity of potent compounds on neuroblastoma cells.

3.2.1.1. Cholinesterase inhibition studies

The ability of the synthesized derivatives (**3**, **6** and **9**) to inhibit both *h*AChE and equine BuChE was evaluated *in vitro* (IC₅₀ values, **Table 6**). They exhibited a broad range of inhibition (AChE IC₅₀ = 4.63 to >100 μ M; BuChE IC₅₀ = 0.093-88.06 μ M). On the other hand it was observed that modification in the ring size of cyclic guanidine decreased the activity (derivatives of compounds **6/9**). Among all of the synthesized compounds (about 75), derivatives of six- membered cyclic guanidine skeleton (2-imino-4-quinazolinones) were found to be most active compounds. It was observed that the activity of compounds bearing cyclic guanidine skeleton was overall

Table 6. AChE and BuChE inhibition and selectivity index of cyclic guanidine motifs

Entry	R ₁	R ₂	IC ₅₀ (μM) ^a		Selectivity index (SI) ^b
			AChE	BChE	
3af			9.1	74.16	0.12
3ai			6.77	22.13	0.30
3al			100	5.56	29.13
3am			100	47.3	--
3an			61.62	0.093	628.77
3bg			14.13	0.098	151.93
3bh			39.13	88.06	0.44
3bi			9.14	29.77	0.30
3bk			4.63	24.1	0.19
3bl			9.14	26.07	0.35
3bm			10.25	17.74	0.57
3bo			45.71	9.08	5.03
3bs			9.15	21.51	0.42
3cf			7.65	32.22	0.23
3ch			20.09	22.84	0.87
3ci			100	11.61	--
3cl			9.72	25.72	0.37
3cn			18.1	25.52	0.70
3dh			16.43	13.14	1.25
3dn			13.7	15.51	0.88
3eh			12.93	26.34	0.49
3ei			6.77	11.46	0.59
3ek			11.02	40.77	0.27
3el			9.47	55.49	0.17
3en			12.95	81.31	0.15
3es			53.66	21.98	2.44
6n	--		30.91	>100	--

6o	--		94.55	>100	--
6s	--		>100	>100	--
9ct			>100	>100	--
9es			90.54	>100	--
Tacrine HCl			0.093	0.019	4.89
Donepezil HCl			0.032	3.60	0.008

^a The *in vitro* test compound conc. required to produce 50% inhibition of *h*AChE and BuChE.

^b The result (IC_{50}) is the mean of two separate experiments ($n = 4$) and the deviation from the mean is <10% of the mean value. Selectivity index = *h*AChE IC_{50} /BuChE IC_{50} .

decreased to almost inactive on increasing the ring size (seven-membered 2-amino-5-tribenzazepinones) or decreasing the ring size (five-membered 2-aminobenzimidazoles). Out of seventy 2-imino-4-quinazolinone (**3**) derivatives about 26 compounds were showing IC_{50} values below 100 μ M concentration and are listed in the **Table 6**. Remaining compounds were found to be very less active or inactive for AChE / BuChE inhibition. Compound (**3bk**) was found to be the most active compound with an IC_{50} value of 4.63 μ M for AChE inhibition. Among all of the tested compounds 19 compounds (**3af**, **3ai**, **3bg**, **3bi**, **3bk**, **3bl**, **3bm**, **3bs**, **3cf**, **3ch**, **3cl**, **3cn**, **3dh**, **3dn**, **3eh**, **3ei**, **3ek**, **3el**, **3en**) have shown good inhibitory activity for AChE inhibition with $IC_{50} \leq 20$ μ M; the other seven compounds (**3al**, **3am**, **3an**, **3bh**, **3bo**, **3ci**, **3es**) have shown moderate inhibitory activity for AChE with IC_{50} values ranging from 20 μ M to 100 μ M. For BuChE inhibitory activity compound (**3an**) was found to be the most active with an IC_{50} value of 0.093 μ M and compound (**3bg**) also demonstrated good BuChE inhibition with an IC_{50} value of 0.098 μ M. Nine out of all of the compounds (**3al**, **3an**, **3bg**, **3bm**, **3bo**, **3ci**, **3dh**, **3dn**, **3ei**) have demonstrated good activity for BuChE inhibition with $IC_{50} < 20$ μ M; rest have shown IC_{50} values in the range of 20-100 μ M. As the aim of the study was to identify new chemical entities for their ChE inhibitory activities with proper selectivity towards AChE and BuChE,

the selectivity index (SI) of active compounds was calculated. SI of compound (**3bk**) was found to be 0.19 towards AChE but SI of compound (**3an**) and compound (**3bg**) was found to be 628.77 and 151.93 respectively for BuChE inhibition. The overall observation of the data demonstrated that compounds having high AChE inhibitory activity are also good inhibitors of BuChE but compounds having high BuChE inhibitory activity were typically more selective for BuChE inhibition.

3.2.1.2. Inhibition of *h*AChE-induced A β aggregation

All the 26 compounds observed to be active for ChE inhibitory activity were also evaluated to prevent *h*AChE-induced A β ₁₋₄₀ aggregation by a thioflavin T (ThT) fluorescence method.⁸⁶ The anti-aggregating activity of nine 2-imino-4-quinazolinone derivatives (**3**) along with the reference compound tacrine are presented in **Table 7**. At a concentration of 100 μ M, 2-imino-4-quinazolinones exhibited varying degrees of

Table 7. Inhibition of *h*AChE-induced aggregation of A β ₁₋₄₀ and MTT reduction cytotoxicity assay in SH-SY5Y neuroblastoma cells of cyclic guanidine motifs

Entry	Inhibition A β ₁₋₄₀ at 100 μ M \pm SEM (%) [*]	Cell viability in SH-SY5Y cells at 80 μ M \pm SEM (%) [*]
3ai	37.10 \pm 1.16	76.81 \pm 10.7
3bk	30.03 \pm 1.16	74.54 \pm 6.56
3bs	22.78 \pm 1.35	64.80 \pm 5.79
3cf	11.86 \pm 1.07	79.49 \pm 7.31
3ch	21.96 \pm 0.98	45.24 \pm 3.32
3cl	12.53 \pm 1.01	94.05 \pm 16.77
3cn	24.76 \pm 0.95	54.96 \pm 15.78
3el	8.350 \pm 0.88	98.57 \pm 18.03
3en	9.723 \pm 0.89	68.42 \pm 7.69
Tacrine HCl	33.82 \pm 1.17	80.24 \pm 1.58

^{*} The values for Inhibition of aggregation of A β ₁₋₄₀ are the mean of two independent measurements each performed in triplicates and the values for MTT assay are the mean of measurements performed in quadruplicates, SEM = standard error of mean. 100% cell viability stands for the viability of SHSY5Y cells measured in the absence of small molecules, as determined by MTT reduction. Statistical analysis using an independent two-tailed student's t-tests were performed using Origin 7.0 (Microcal Software, Inc., Northhampton, MA) to evaluate the statistical significance of the difference between the viability of control cells (measured in the absence of test molecules) and experimental mean values. A *p*-value of <0.05 was defined as statistically significant.

inhibition. Out of all of the screened compounds, nine derivatives (**3ai**, **3bk**, **3bs**, **3cf**, **3ch**, **3cl**, **3cn**, **3el** and **3en**) have demonstrated promising activity. Compound (**3ai**) was found to be the most active with 37% inhibition of aggregation which is in resemblance or slightly better than the reference compound tacrine (33% inhibition). Compound (**3bk**) the most active compound for ChEI activity is also showing the A β -aggregation inhibition which proved the hypothesis of dual activity of test compounds as ChE inhibitors and A β -aggregation inhibitors.

3.2.1.3. SH-SY5Y neuroblastoma cell toxicity

The cytotoxicity of 2-imino-4-quinazolinone derivatives (**3ai**, **3bk**, **3bs**, **3cf**, **3ch**, **3cl**, **3cn**, **3el** and **3en**) was evaluated using a 3-(4,5-dimethylthiazol-2-yl)-2,5-diphenyltetrazolium bromide (MTT)-based colorimetric assay. The cell viability of SH-SY5Y neuroblastoma cells after exposure to 2-imino-4-quinazolinones was compared with reference compound tacrine (**Table 7**). At 80 μ M, all of the tested quinazolinone derivatives (**3**) maintained efficient cell viability as measured by MTT reduction and were relatively nontoxic (**Table 7**). The isopropyl derivative (**3ai**) that exhibited selective AChE inhibition ($IC_{50} = 6.77 \mu$ M) and excellent anti-aggregation activity (37% inhibition) was very less toxic (76% cell viability). For comparison, the viability of SH-SY5Y cells was 80% in the presence of the reference compound tacrine under the same experimental conditions. In addition, the cyclopropyl derivative (**3bk**) (most potent AChEI, $IC_{50} = 4.63 \mu$ M and 30% inhibition of A β -aggregation) was only slightly toxic under these conditions, with cell viabilities of 74%. The *n*-butyl derivative (**3ch**) was found to be more than 50% toxic to the neuroblastoma cells and rest other compounds were significantly safe as indicated by

cell toxicity assay. On the basis of data obtained after cytotoxicity studies it could be concluded that the 2-imino-4-quinazolinone derivatives were nontoxic or only slightly toxic to SH-SY5Y cells and could serve as a suitable template to develop ChEIs that exhibited activity against AChE-induced aggregation of A β .

3.2.1.4. Molecular modeling (docking) studies

Human acetylcholine esterase (*hAChE*) has two major binding sites, one is peripheral anionic site (PAS) and the other is catalytic active site (CAS) which is deeply located in the structure and is assigned with Ser-His-Glu catalytic triad.

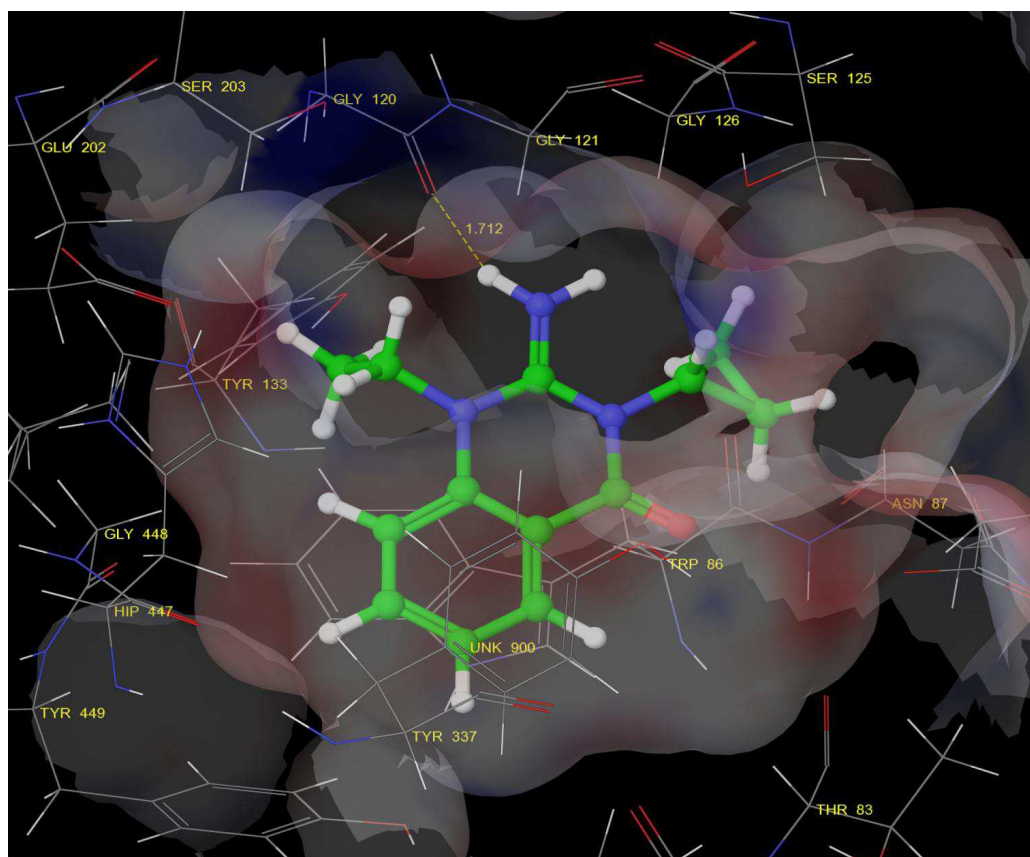


Figure 7. *hAChE* docked with compound (3bk)

Among all of the synthesized compounds, ligand interaction with receptor (PDB Code: 1B41) by means of docking for the most active compound (**3bk**) is discussed here (**Figure 7**). The compound (**3bk**) deeply fits in the CAS, and located at ~ 13 Å from the Trp-286 of PAS and ~ 7 Å from the catalytic triad His-447 which resides at the bottom of active site gorge. The imino N-H stabilizes the complex by forming hydrogen bond interaction with Gly-120 (1.71 Å). Cyclopropyl ring appears towards the PAS. Iminoquinazolinone ring system is equidistantly (~ 4.5 Å) located in between Tyr-337 and Trp-86 and exhibits *pi-pi* stacking interaction of iminoquinazolinone aromatic part with Tyr-337 and Trp-86.

A similar docking experiment was conducted within the active site of *h*BuChE

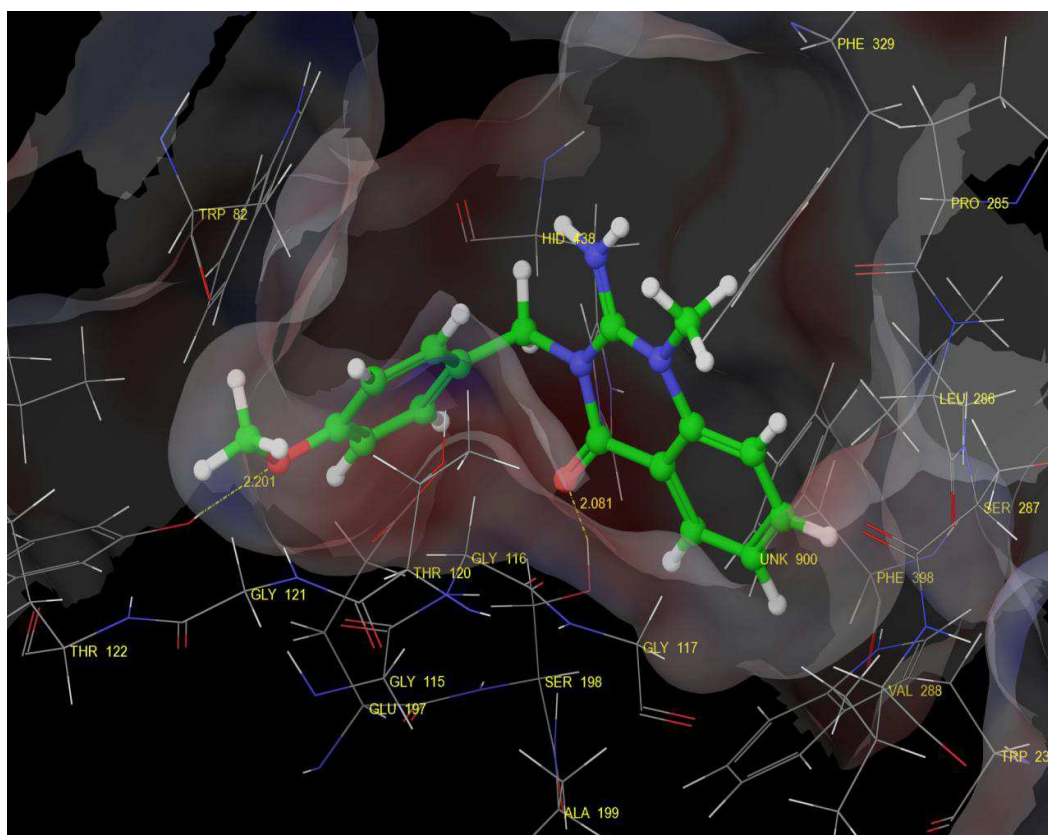


Figure 8. *h*BuChE docked with compound (**3an**)

(PDB Code: 1P0I) with the most potent BuChE inhibitor (**3an**) (**Figure 8**). This study indicated that methoxyphenyl is aligned close to the hydrophobic pocket Gly-115–117 (~4.5 Å). Aromatic ring of methoxyphenyl is oriented parallel to Trp-82 and is imparting good hydrophobic interaction. Further, methoxy group stabilizes ligand receptor interaction by forming hydrogen bond with Tyr-128 (2.20 Å). The carbonyl group of iminoquinazolinone is oriented towards the Ser-198 and His-438. It has demonstrated hydrogen bonding interaction with Ser-198 (2.08 Å) and the aromatic ring of iminoquinazolinone has been found to be oriented towards aromatic cage comprising of Trp-231, Phe-329 and Phe-398.

The screening data (**Table 6**) demonstrated that the ring size of cyclic guanidine motif was the most important factor for the activity of guanidine derivatives. Among the three scaffolds only the six-membered (2-iminoquinazolin-4-one) was found to provide active compounds. Increasing or decreasing the ring size of cyclic guanidine motif resulted in overall decrease in activity and this result is supported by molecular docking studies also, as six membered ligands fitted deeply into the catalytic active site (CAS) of ChE crystal structure. Structure–activity relationship (SAR) studies indicated that the cholinesterase inhibition and selectivity were sensitive to steric and electronic parameters at N-1 and N-3 positions of the central quinazolinone ring. The most active compound (**3bk**) for AChEI activity, had cyclopropyl substituent at N-3 position and ethyl substituent at N-1 position. In general, compounds with ethyl substituent at N-1 position (**3bg**, **3bh**, **3bi**, **3bk**, **3bl**, **3bm**, **3bo** and **3bs**) acquired good activity for AChEI. At N-3 position compounds having cyclopropyl substituent (**3bk** and **3ek**) demonstrated very good activity for AChEI. The observation matched with docking studies as cyclopropyl ring appeared at peripheral anionic site (PAS). The

isopropyl substituent at N-3 position (**3al**, **3bi** and **3ei**) also demonstrated good AChEI activity except for compound (**3ci**). Increasing the chain length at N-3 position from propyl to butyl (**3bh**, **3ch** and **3eh**) caused the AChEI activity to slightly decrease. Introducing the aromaticity at N-3 position (**3am**, **3an**, **3bo**, **3cn**, **3dn**, **3en** and **3es**) in general slightly decreased the AChEI activity but in compounds (**3bm** and **3bs**) the activity did not decrease because of ethyl substituent at N-1 position. Apart from other substituents, allyl and benzyl substituents at N-1 position did not make any significant change in AChEI activity of the compounds. On the other hand substituents with aromatic character made significant changes in BuChEI activity of compounds; activity was increased in general especially in the case of *p*-methoxybenzyl substituents (**3an**, **3cn**, **3dn** and **3en**). Docking studies also suggested that the methoxyphenyl ring had good hydrophobic interactions with the active sites of *h*BuChE. The most active compound (**3an**) for BuChEI activity had a methoxybenzyl substituent at N-3 position and methyl substituent at N-1 position. It was also observed that the compounds which are more active towards BuChEI activity demonstrated very high selectivity (**3an** and **3bg**). As it has been previously mentioned that during the initial stages of AD the prevalence and role of AChE is highly dominating but at advanced stage or in later days of AD the prevalence and activity of BuChE increases significantly, as a result A β -aggregation increases. Keeping these facts in mind the designing of NCEs could be directed in that direction i. e. in the initial stage of AD treatment targeting AChE and BuChE should be given and at a later stage more selective treatment of BuChEI should be used. The active compounds obtained at the end of this study could be used in both stages, compound (**3bk**) in the initial stage and compound (**3an**) in the advanced stage of AD.

3.2.2. Part B-Anti-thrombotic activity

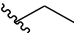
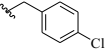
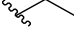
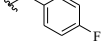
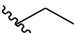
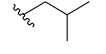
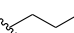
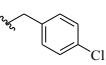
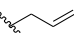
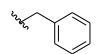
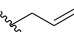
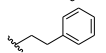
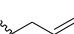
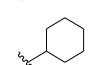

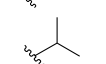
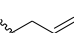
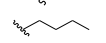
The discovery of orally active, small molecule competitive fXa inhibitors in preclinical animal thrombosis models in recent years has spurred the process for discovery of such molecules as anti-thrombotic drugs. Survey of literature revealed carboxamides and anthranilamides to possess either fXa inhibitory activity or anti-platelet aggregating activity.⁸⁷ Betrixaban, an anthranilamide derivative, is a proven orally active fXa inhibitor useful in prevention of thromboembolic events.⁸⁸ It has undergone human clinical trials for prevention of embolism after knee surgery and prevention of stroke following atrial fibrillation⁸⁹ with promising results.⁹⁰ Taking betrixaban as the lead molecule it was planned to substitute both the nitrogens with various alkyl/aryl substituents to provide compounds of type (2). It has been revealed earlier that some compounds exhibiting very high *in vitro* antithrombotic activity failed to produce the desired effect when administered orally. As the designed compounds (2) were expected to possess anti-platelet and/or anticoagulant activity it would require a battery of *in vitro* tests to be performed to assess the compounds for these activities. For anti-platelet activity, the compounds need to be evaluated against a multitude of agonists like ADP, AA, PMA, A23187, collagen and thrombin. Separate tests need to be performed for anticoagulant and thrombolytic activities as many proteases are involved in the activation of coagulation cascade. Moreover it is difficult to test hydrophobic samples as methanol/DMSO could not be used for solubilisation of these samples as both the solvents are potent inhibitors of platelet activation. Realising the complexity of the problem it was planned to assess antithrombotic efficacy of the synthesized compounds after oral administration as that

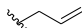

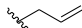
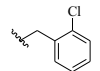
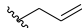
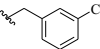
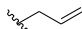
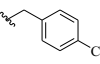
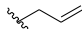
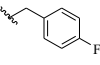
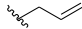
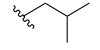
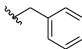
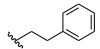
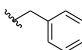
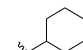
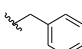

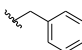
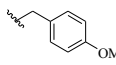
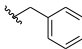
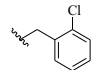
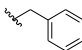
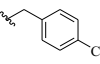
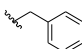
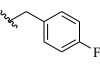
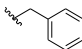
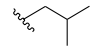
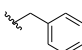
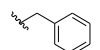
would exhibit the overall effect of the compounds on platelets as well as coagulation cascade after oral absorption.

3.2.2.1. Evaluation of anti-thrombotic activity after three days treatment

A simple, reliable and reproducible animal model was used to assess the antithrombotic activity of the synthesized compounds. Bleeding time was used as a parameter to have an idea of their effect on hemostasis at a particular dose. Experiments were conducted to evaluate the *in vivo* effects of the synthesized compounds on antithrombotic activity,⁹¹ bleeding time⁹² and prothrombin time (PT),⁹³ in mice. The compounds were suspended in 0.5% aqueous CMC (sodium carboxymethyl cellulose) and administered orally. Warfarin as reference compound

Table 8. *Ex-vivo* assay of novel 2-aminobenzamide derivatives (**2**) for antithrombotic activity, bleeding time and prothrombin time after three day treatment at dose of 30 μ M/kg.

Entry	R ₁	R ₂	AA (% protection)	BT (% increase)	PT (sec.)
Control	--	--	--	--	12.2
2bq			40	100	9.5
2br			40	55	11.0
2bj			23	100	11.4
2cq			42	100	9.5
2dm			32	91	11.9
2ds			30	63	9.3
2dl			26	55	10.2
2di			20	65	11.6
2dh			23	68	9.4

2dk			20	44	10.2
2do			42	82	10.0
2dp			40	70	10.2
2dq			42	68	8.5
2dr			44	55	11.4
2dj			26	50	11.0
2es			40	82	8.7
2el			30	109	9.7
2ek			26	36	10.6
2en			48	45	11.2
2eo			44	65	10.5
2eq			40	68	10.3
2er			46	55	11.1
2ei			34	100	9.9
2em			38	62	10.2
Warfarin	--	--	50	45	118.2

(AA) Antithrombotic Activity; (BT) Bleeding Time; (PT) Prothrombin Time;
Control = 0.5% aqueous CMC

was tested under the same conditions and the results are presented in **Table 8**. Out of all of the compounds evaluated for activity, twelve compounds showed 40% or higher antithrombotic activity, while remaining compounds exhibited activity between 20-40%. The most promising one was compound (**2en**), showing antithrombotic protection of 48% (warfarin under similar conditions showed 50% protection); but at variance with warfarin, **2en** exhibited a low PT of 11.2 min as against 118.2 min for

warfarin, suggesting that the mechanism of the newly synthesized compounds might be different.

3.2.2.2. Evaluation of anti-thrombotic activity after one hour treatment

Next, the synthesized compounds were evaluated using aspirin as standard drug and the results are presented in **Table 9**. Nine of the compounds (**2cq**, **2en**, **2eo**, **2eq**, **2er**, **2do**, **2dp**, **2dq** and **2dr**) showed comparable antithrombotic activity to the standard drug aspirin. Tolerability of the sub-acute treatment with the compounds was examined by evaluating their adverse pro-hemorrhagic effect on tail bleeding time. Again, compound (**2en**) emerged as the most promising one, because in addition to showing 42% protection, it did not increase the bleeding tendency substantially in comparison to aspirin at its optimal antithrombotic dose. Although the other active compounds exhibited good protection but they also caused increase in bleeding time, which was a drawback.

Table 9. *Ex-vivo* assay of novel 2-aminobenzamides (**2**) for antithrombotic activity as well as bleeding time after one hour treatment at dose of 30 μ M/kg

Entry	AA (% protection)	BT (% increase)	Entry	AA (% protection)	BT (% increase)
2bq	35	48	2dr	30	44
2br	30	45	2dj	20	25
2bi	20	17	2es	30	58
2cq	30	83	2el	20	34
2dm	20	38	2ek	10	32
2ds	20	17	2en	40	23
2dl	20	58	2eo	40	59
2di	20	50	2eq	40	60
2dh	20	34	2er	40	75
2dk	10	25	2ei	30	33
2do	40	100	2em	30	52
2dp	30	36	Aspirin	37 \pm 3	100 \pm 20
2dq	30	20			

3.2.2.3. Acute oral toxicity study in mice

The *in vivo* toxicity study was also performed for the compounds (**2en**, **2eo**, **2er** and **2dr**). For all of the test compounds (**2en**, **2eo**, **2er** and **2dr**) the LD₅₀ was found to be >2000 mg/kg. At a limiting dose of 2000 mg/kg body weight, **2en**, **2eo**, and **2er** did not show any toxicity signs on the day of dosing and during the 14 day observation period. Compound (**2dr**) showed toxicity sign in one of the animals out of three. The study was repeated at a dose of 2000 mg/kg for compound (**2dr**) and again one animal out of three showed toxicity signs. Further, histological analysis of the major organs like liver, kidney, heart, brain and stomach was performed. As shown in **figure 9a** treatment with **2dr** induces hepatic microgranulation as compared to the vehicle treated animal (**figure 9b**). While other organs i.e. kidney (**Figure 10a-b**), heart (**Figure 1a-b**), stomach (**Figure 12a-b**) and brain (**Figure 13a-b**) did not show any toxicity signs in histopathological examination. The principal mechanism for histological injury in liver still remains to be clarified. The results of acute toxicity study made it obvious that compounds (**2en**, **2eo**, and **2er**) at a limiting dose of 2000 mg/kg body weight were not lethal. So the LD₅₀ of these compounds were >2000 mg/kg, while compound (**2dr**) was lethal for one animal out of three. According to guideline, compound (**2dr**) could be placed in category 5 and it could be concluded that LD₅₀ of **2dr** is >2000 mg/kg. Considering the administering dose of only 1-10 mg/Kg for the desired biological activity (i. e. anti-thrombotic activity), the therapeutic window of synthesized compounds (**2**) is very wide.

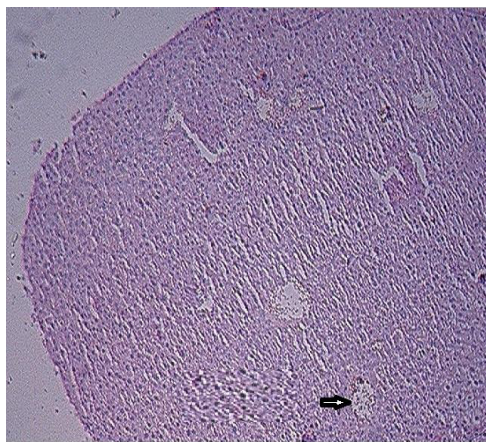


Figure 9a. Compound (2dr) treated Liver

- Black arrow in **figure 9a** is showing microgranulation

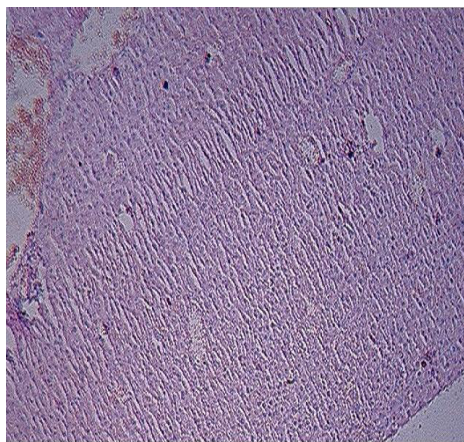


Figure 9b. Vehicle treated Liver

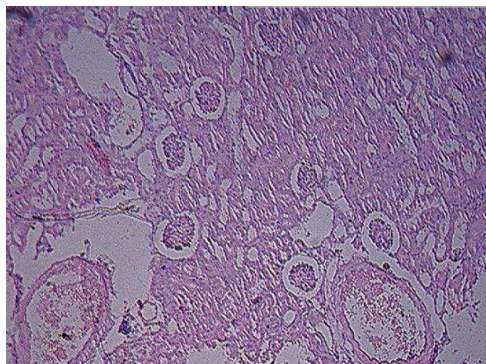


Figure 10a. Compound (2dr) treated Kidney

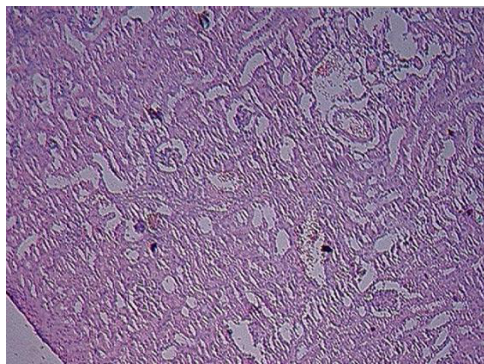


Figure10b. Vehicle treated Kidney

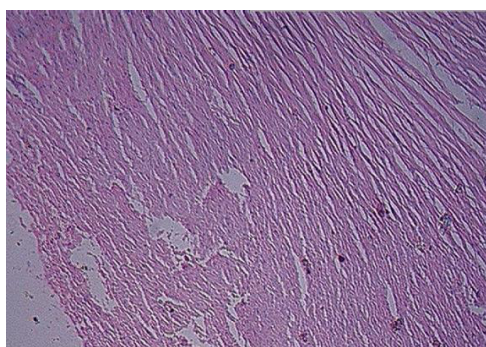


Figure 11a. Compound (2dr) treated Heart

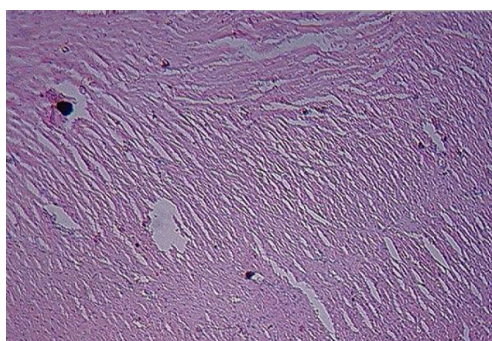
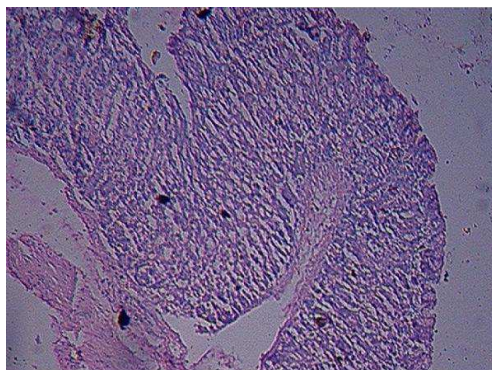


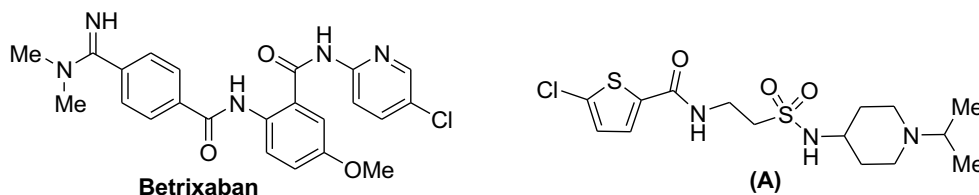
Figure11b. Vehicle treated Heart

**Figure 12a.** Compound (2dr) treated Stomach**Figure12b.** Vehicle treated Stomach**Figure 13a.** Compound (2dr) treated Brain**Figure13b.** Vehicle treated Brain

3.2.2.4. Molecular modeling (docking) studies

As fXa is responsible for thrombotic activity ultimately, it was thought of studying the binding interactions of the active compounds using crystallographic 3D structure of fXa. Factor Xa is having well identified active site with mainly four recognized regions. It has S1, S2, S4 and an ester binding pocket (EBP) in the active binding space. Among these S1 and S4 sites are more important for ligand binding and exhibiting the biological activity. S2 is a small pocket separated from S4 by Tyr 99.⁹⁴ Extra precision (XP) docking studies were performed for the compounds under investigation. To validate the docking studies under the Glide tool of Schrödinger

2009⁹⁵ environment, the co-crystallized molecule (**A**) present in the 3D structure of fXa (PDB Code: 4A7I) was first knocked out of the binding site. The molecule was constructed again, energy minimized and re-docked into the active site of the enzyme. Very similar interactions were observed between the re-docked molecule and the enzyme as was observed in the original co-crystallized structure i.e. similar orientations of the groups in S1 and S4 binding pockets and binding interactions with Tyr-228, Gln-192 and Gly-216 were observed. The root mean square deviation between the predicted conformation and the original conformation of compound (**A**) as existed in the X-ray crystallographic structure was found to be 0.26 Å. The interm-



-olecular docking interactions of the most active compound (**2en**) are shown in **Figure 9**. It is clearly observed that occupying of S1 and S4 sites by specific lipophilic functionalities is very important for greater binding affinity of the ligands with the enzyme. To establish probable mechanistic orientation of the synthesized molecules the intermolecular interactions of the lead molecule betrixaban was compared with the docking interactions of the most active compound (**2en**). In compound (**2en**), phenyl ring of the N-benzyl group fits in S1 pocket indicating good lipophilic interaction while in betrixaban pyridine ring shows similar interaction in addition to the non-covalent lipophilic interaction between -Cl of pyridine and pi-system of Tyr-228 of S1

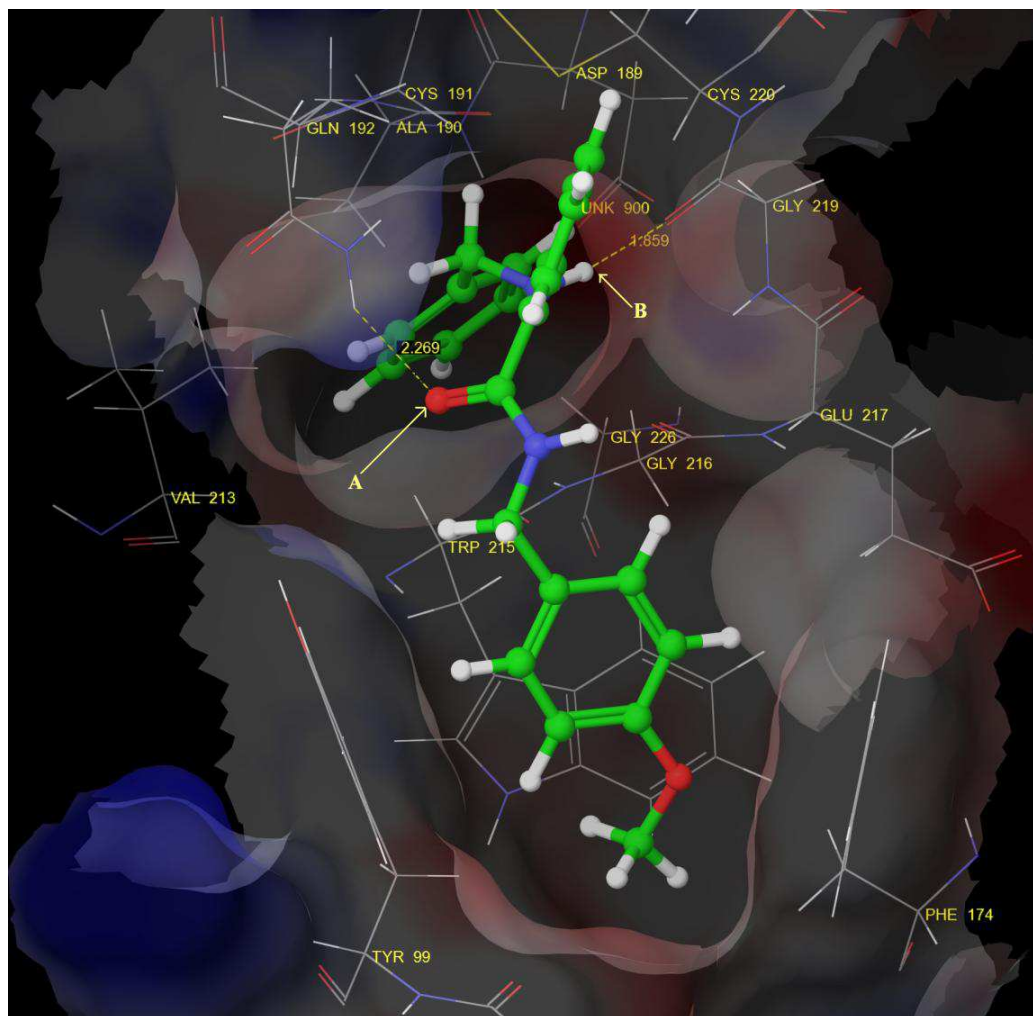


Figure 9 Compound (**2en**) docked into the active site of fXa (Pointer A and B showing H-bonding with Gln-192 and Gly-219 respectively)

pocket. Here -Cl is placed 3.8 Å away from centroid of Tyr-228 aromatic ring. The amino NH of compound (**2en**) stabilizes the complex by forming hydrogen bond with -C=O of Gly-219 (1.8 Å). Whereas in betrixaban pyridine amide NH stabilizes the complex by hydrogen bonding with -C=O of Gly-219 (2.1 Å) and with disulphide linkage of Cys-191 and Cys-220 (2.4 Å). The methoxyphenyl component of compound (**2en**) fits into the S4 binding pocket with centroid to centroid distance of 4.6 Å, 4.3 Å and 5.1 Å from the phenyl ring of methoxybenzyl moiety to the aromatic

rings of Tyr-99, Trp-215 and Phe-174 respectively. The amide --C=O of our compound (**2en**) interacts with NH of Gln-192 by forming a hydrogen bond (2.26 Å). While in case of betrixaban, the *N,N*-dimethylcarbamimidoyl benzoyl part fits in the S4 binding pocket with centroid to centroid distance of 4.47 Å, 5.60 Å and 6.35 Å between aromatic ring of this part and aromatic rings of Tyr-99, Trp-215 and Phe-174 respectively. From this part of betrixaban the --C=O and NH of amide shows hydrogen bonding interaction with NH of Gln-192 (2.35 Å) and --C=O of Gly-216 (1.90 Å) respectively.

A look at **Table 8** revealed that alkyl substituents at both the nitrogens [amine NH (R_1) and amidic NH (R_2)] offered compounds (**2dl**, **2di**, **2dj**, **2dh** and **2dk**) having increased bleeding time but poor anti-thrombotic activity. This is in consonance with the docking studies wherein poor interactions of both of the alkyl groups in S1 and S4 pockets were observed. Replacement of the alkyl groups at the amidic ‘N’ or the amine ‘N’ by benzyl/substituted benzyl (**2bq**, **2br**, **2es**, **2el**, **2ek**, **2ei**, **2dm**, **2do**, **2dp**, **2dq**, **2dr**, **2cq**) led to an increase in anti-thrombotic activity with moderate to high enhancement in bleeding time. Substitution of the alkyl groups at both the nitrogens with benzyl/substituted benzyl groups offered compounds (**2en**, **2eo**, **2eq** and **2er**) with improved anti-thrombotic activity. Both of these observations are supported by the docking studies. Simultaneous substitution of both the nitrogens with benzyl/substituted benzyl group yields compounds having much better interactions with the enzyme in both of the vital binding pockets S1 and S4. 4-Methoxybenzyl substituent (**2en**) at amide nitrogen with a benzyl group (R_1) at amine nitrogen is responsible for increase in anti-thrombotic activity with negligible effect on PT. Replacement of 4-methoxyphenyl with halo substituted phenyl ring maintained the

anti-thrombotic activity in the resulting compounds (**2eo**, **2eq** and **2er**) but it led to increase in the bleeding time also. Among the halo derivatives, the fluoro- derivative (**2er**) offered the best biological activity profile. For the purpose of comparative study compound (**2em**)⁹⁶ having benzyl substituents at both the nitrogens was synthesized and biologically evaluated. In the docking studies also it was observed that a lipophilic substituent at 4-position of amidic benzyl ring was essential for lipophilic interaction in S4 pocket of the enzyme with the ligand. It seems substitution of benzyl/substituted benzyl in place of alkyl/cycloalkyl groups at amidic 'N' (**2bq**, **2br**, **2do**, **2dp**, **2dq**, **2dr**, **2cq**) has more profound impact on anti-thrombotic activity than the substitution of benzyl group on amino 'N' (**2el**, **2ek**, **2ei**). It is interesting to note that the newly reported compound (**2en**) did not cause increase in bleeding time or PT at variance with aspirin or warfarin at anti-thrombotic doses, while maintaining almost same anti-thrombotic activity as warfarin. These observations point out that derivative (**2en**) has the potential to provide a better therapeutic window over warfarin and aspirin.